Fully Automated Bi-Hormonal Intraperitoneal Artificial Pancreas Using a Two-Layer PID Control Scheme

Jana Langholz, Karim Davari Benam, Bindu Sharan, Sebastien Gros, Anders Lyngvi Fougner

***Abstract*—Treatment of type 1 diabetes mellitus is significantly improved by using commercially available hybrid closed-loop systems to deliver insulin. These systems, also called artificial pancreas (AP), use the subcutaneous (SC) route to deliver insulin. However, meal announcements are necessary due to the slow insulin absorption from the SC tissue. Thus due to the need for human intervention, it is called "hybrid closed loop" AP. In this work, a bi-hormonal AP with intraperitoneal (IP) infusion is designed to increase the time within the range of 3.9–10.0 mmol/l and alleviate the burden of meal announcements. A two-layer controller is designed to provide safe and effective insulin and glucagon delivery. The primary layer is based on classical PID controllers for insulin and glucagon, and the supervisory layer includes four parts: (A) Zone-based control settings, (B) Extrapolation of sensor data to compensate for sensor delay in SC tissue, (C) Auto-tuning of the PID parameters in the primary layer through simulation in an animal model, and (D) Safety barriers. The controller is designed to prevent hypoglycemia after meals and during physical activity, as well as prevent postprandial hyperglycemia. The designed AP achieved 92.5% of the time within the range of 3.9–10.0 mmol/l on a simulator trained on data from animal experiments. The results indicate that this two-layer control structure with IP infusions makes it feasible to achieve a fully automated artificial pancreas without the need for meal announcements, i.e. without human intervention.**

I. Introduction

Patients with type 1 diabetes depend on exogenous insulin since their insulin-producing β-cells are destroyed or are not able to produce enough insulin. As a result, the body fails to control the Blood Glucose Level (BGL) [1]. Current diabetes treatment consists of three stages; First, the BGL must be measured, then the amount of the necessary hormone must be determined, and finally, this amount must be injected. The automated system that can perform these procedures is called the artificial pancreas (AP). Commercially available AP systems include a control system to determine the amount of insulin, a pump for injecting the insulin into the subcutaneous (SC) tissue, and a blood glucose sensor for measuring the BGL [2].

Due to the slow insulin absorption from the SC tissue, most control approaches fail to keep the BGL within the desired range when facing an unannounced meal [3]. Notably, the meal announcements need to be done by the patients well in advance. Otherwise, a delayed meal announcement or underestimated size of the meal can cause hyperglycemia (high BGL). Hyperglycemia is caused by too little (or no) meal insulin or the meal insulin being given too late relative to the meal. If hyperglycemia occurs often, the patient will have a higher risk of microvascular complications and cardiovascular diseases. Improved glycemic control alleviates these risks.

On the other hand, an overestimated meal size can cause hypoglycemia (low BGL). Since hypoglycemia can have serious short- and long-term implications, it is a critical occurrence that must be avoided. As categorized later in Table II by the American Diabetes Association, the first level of hypoglycemia is set at a threshold where neuroendocrine response starts failing. However, the symptoms can be unrecognized, and for that reason, the risk of experiencing hypoglycemic unawareness exists. In the second level, neuroglycopenic symptoms arise, and immediate actions should be taken. If it stays untreated, the patient can experience significant changes in mental and physical functioning, progressing further into consciousness, seizure, coma, or death [1, Chapter 6].

It has been shown in [3] that the intraperitoneal (IP) route has a faster insulin absorption than the SC route, and the AP systems using the IP route do not need the meal announcements. In addition, bi-hormonal AP systems are shown to be effective in avoiding hypoglycemia [4]. Bi-hormonal AP uses a second hormone next to insulin to increase the BGL. This hormone, called glucagon, can stimulate the breakdown of glycogen into glucose in the liver. Thus, glucose is accessible in case of need for energy [5].

Several studies have been done in the literature to design different controller approaches, such as Model predictive control (MPC) and PID controller for single hormonal SC AP [6]–[8]. In addition, a few other research groups are focusing on bi-hormonal SC AP [9]–[11] showing more promising results than single-hormonal APs. However, few controllers have been tested and designed for single hormonal IP AP without meal announcements. This is due to the lack of a simulator for the IP insulin and glucagon infusion. Nonetheless, Toffanin *et al.* in [3] used an MPC approach to control the BGL for single hormonal IP AP, where they used a modified version of the SC simulator. The results showed that IP insulin does not require meal announcement. Huyett *et al.* in [12] used a simulator with intravenous (IV) insulin infusion and assumed that IP and IV insulin infusions have the same

This research is funded by the Research Council of Norway (project no. 248872), and the Centre for Digital Life Norway.

J. Langholz, and B. Sharan are with Institute of Control Systems, Technical University of Hamburg, Eißendorfer Straße 40, 21073 Hamburg, Germany. {jana.langholz, bindu.sharan}@tuhh.de

K. D. Benam, S. Gros, and A. L. Fougner are with Department of Engineering Cybernetics, Faculty of Information Technology and Electrical Engineering, Norwegian University of Science and Technology (NTNU), O. S. Bragstads Plass 2D, 7034 Trondheim, Norway. {karim.d.benam, sebastien.gros, anders.fougner}@ntnu.no

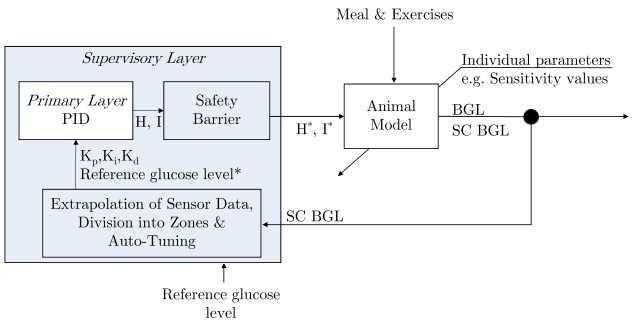

Fig. 1: Block diagram of the proposed two-layer control structure. The primary layer consists of two PID controllers for insulin and glucagon infusions. The supervisory layer manages the safety barriers, extrapolates the sensor data to compensate for the sensor delay, and modifies the set points and PID coefficients in accordance with the BGL values. The inputs to the primary layer are the auto-tuned gains for the controller, the reference BGL of the active zone, the output insulin (I), and glucagon (H). After the safety barrier, the output might be modified, shown by the superscript *. Meal & Exercises are implemented as glucose infusion rates in the simulator. The simulator outputs are blood glucose level (BGL) and the subcutaneously BGL (SC BGL) measurement.

absorption rates. Then, they designed a PID controller for insulin infusion using the sensors inside the peritoneal cavity. The results showed significant improvements in simulations.

This paper thereby focuses on designing the control algorithm for a bi-hormonal IP AP. To this end, a two-layer control structure is developed and tested on the simulator. As shown in Fig. 1, the primary layer includes two PID controllers for insulin and glucagon, respectively; at every instant only one of them is activated by the supervisory layer depending on the BGL and its derivative. In addition, reference BGL and PID coefficients are specified by the auto-tuning algorithm in the supervisory layer. Moreover, the supervisory layer is responsible for safety barriers, emergency modes, and compensating for sensor delays.

The proposed control structure is tested on a simulator which was trained/identified based on data from 13 animal experiments [13]. The controller was exposed to scenarios aiming for typical real life conditions, e.g., with meals, physical activity, sleep, and model mismatch (tuning the controller for a model that does not match perfectly the simulator it was tested on, e.g., by making a time varying insulin sensitivity). To the best knowledge of the authors, the design and test of a bi-hormonal IP AP on a simulator trained and tested for the IP route is novel.

The paper is structured as follows. First, the simulator used to develop the control structure is described in Section II. Then the different stages of the proposed control structure are presented in Section III. Different metrics are employed to assess the proposed controller, and they are introduced in Section IV. The performance of the controller is assisted in different scenarios in Section V. Finally, these results are discussed in Section VI, and a conclusion is given in Section VII.

II. Simulator and Scenarios

The development and evaluation of the proposed control structure take place in a simulator. To the authors' best knowledge, the proposed "meta model" in [13] is the only model available for testing a bi-hormonal IP artificial pancreas. Other models in the literature are developed for IP routes, but they are designed only for control purposes and have simple pharmacokinetics and pharmacodynamics to serve as a simulator [14], [15]. The meta model is generally based on physiology, and its parameters are identified empirically through 13 experiments in anesthetized pigs, making it a suitable option for a simulator.

The control inputs of the meta model are IP insulin and IP glucagon. IV glucose infusion is used as an additional input to mimic the intestines in anesthetized pigs that absorb glucose, but this input is hidden for the controller. It is used to design challenges (such as meals and exercise) for the controller.

There are only five parameters that must be identified for each new subject:

- The insulin-independent glucose uptake rate (α_1)
- The liver's sensitivity to insulin (α_2)
- The sensitivity of other organs to insulin (α_3)
- The liver's sensitivity to glucagon (α_4)
- The liver's initial glycogen storage level (α_5)

These parameters are unknown to the controller and the sensitivity parameters ($\alpha_2, \alpha_3, \alpha_4$) can vary over time. In [13], the ranges of these parameters are identified based on the animal experiments as follows:

$$\alpha_2 \in [0.57, 5.84], \tag{1a}$$

$$\alpha_3 \in [4.92, 17.22], \tag{1b}$$

$$\alpha_4 \in [6, 20]. \tag{1c}$$

These ranges are used for challenging the controller with different scenarios in which the sensitivities vary. The other parameters of the meta model are population parameters, which are already identified and known using the information from the previous experiments on different subjects.

The simulator was combined with a subcutaneous sensor model that provides a BGL with a time lag as in actual APs. The inputs and outputs of the simulator are illustrated around "animal model" in Fig. 1. The meta model is thereby the basis of the simulator. Insulin and glucagon are the control inputs, meals and physical activity are unknown to the system and thus can be seen as disturbances, the individual parameters are modifiable internal parameters, and actual BGL and subcutaneous BGL (SC BGL) are the output values. To simulate the SC BGL time lag, we used a first order derivative model with parameters (See equation (7) in [16]). Similar to most commercial AP systems, the sampling time of 5 min is chosen for the simulator.

A. Sensitivity to Insulin and Glucagon

As mentioned earlier, the sensitivities of the patient to insulin and glucagon are time-varying parameters. They are influenced by various hormones and conditions, which can affect AP performance. Since determining the sensitivity related to hormones is not straightforward, different modeling possibilities are presented in this section to provide realistic challenges to the controller.

To this end, three different modes are introduced in Fig. 2: The first mode represents the constant value identified during the 13 animal experiments [13]. The second mode is a sinusoidal variation representing fluctuations of sensitivities during the a day. Lastly, a sawtooth profile is used to examine the reaction of the controller to discontinuities due to e.g., a replacement of the infusion set, which would typically happen every 2-3 days in a clinical study. In these simulations, the frequency was increased to make it even more challenging for the controller. For modes 2 and 3, a counteracting effect for insulin sensitivity and glucagon sensitivity is implemented using a phase shift. For example, for mode 2, a phase shift of $90°$ is used. The designed scenario ensures the most significant challenge for the controller because this emulates the fact that when insulin has a high effect on BGL, the glucagon will have the lowest effect, and thus the rescue process is prolonged.

A sinusoidal and sawtooth profile oscillate around a neutral position. Three different neutral positions c_{np} are defined, given by

$$\text{max: } c_{np,max} = b_u - (b_u + b_l) \cdot \frac{v_r}{2} \tag{2a}$$

$$\text{cen: } c_{np,cen} = b_u - (b_u + b_l) \cdot \frac{1}{2}, \tag{2b}$$

$$\text{min: } c_{np,min} = b_l + (b_u + b_l) \cdot \frac{v_r}{2}, \tag{2c}$$

where b is defined as boundary value with either index u as upper or index l as lower value of the regions from (1a)–(1c). The variable $v_r \in [0, 100]\%$ ensures that the sensitivity always stays within the regions, no matter which setting is chosen. The amplitude a is defined as

$$a = (b_u - b_l) \cdot \frac{v_r}{2}. \tag{2d}$$

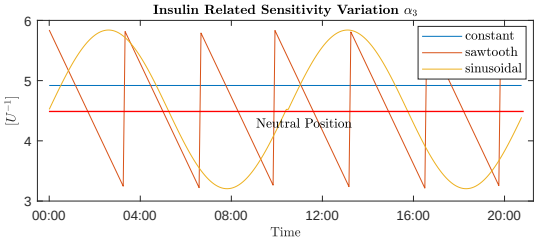

Fig. 2: Visualisation of modes for time-variant hormone sensitivity (using the insulin sensitivity as an example).

B. Glucose Infusion

As described in [13], the meal and exercises can be simulated by the glucose infusion rate R_g in anesthetized pigs. In addition, according to [17], the basal rate of glucose production in adults is between 2–8 $[\frac{\text{mg}}{\text{min}\cdot\text{kg}}]$. In this paper, we assumed that the basal glucose infusion rate is 5 $[\frac{\text{mg}}{\text{min}\cdot\text{kg}}]$, and it is constant in the simulations.

For modeling different realistic scenarios of glucose infusion, basal glucose production can be taken as a basis. To model the food intake of a normal day, different events such as breakfast, lunch, and dinner, as well as soft drinks, can be taken into account, with different amounts resulting in an increase in the glucose infusion rate. Additionally, physical activities can be modeled by decreasing glucose production below basal glucose in anesthetized pigs. The realistic scenario considered to challenge the controller is shown in Fig. 3. The profile of the glucose infusion rate through the day is generated based on the intestine model ("model 2") proposed in [18].

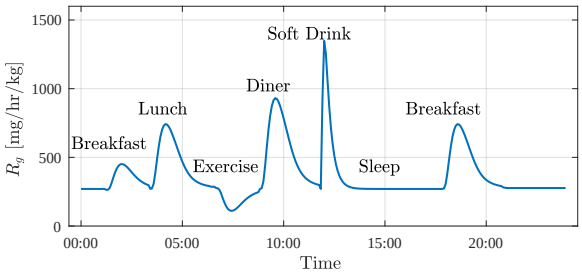

Fig. 3: A demonstrative example of an IV glucose infusion rate in 24 hr to simulate a real-life scenario. Exercise is simulated by reducing the glucose infusion, since it is impossible to perform exercise in anesthetized pigs. The x-axis shows the time (in HH:mm format) since the start of the experiment of the experiment.

III. Two-Layer PID Control Scheme

With the control of the BGL we want to ensure that the BGL is within the target region most of the time. Additionally, the requirement is set to lower or increase the BGL in a safe way. This is because too much glucagon or insulin injection could lead to a dangerous drop or increase of the BGL and can cause severe side effects. Furthermore, oscillations are unwanted, and the amount of injected glucagon should be as low as possible. Therefore, a supervisory layer is implemented to ensure these requirements are met.

There are four different stages implemented in the supervisory layer. The first stage is sensor data extrapolation, the second is dividing the BGL into different zones, the third is the auto-tuning of the PID coefficients in the defined zones, and the last stage is implementing the safety barriers. The designed control scheme is shown in Fig. 4, and the defined stages are explained in more detail in the following subsection.

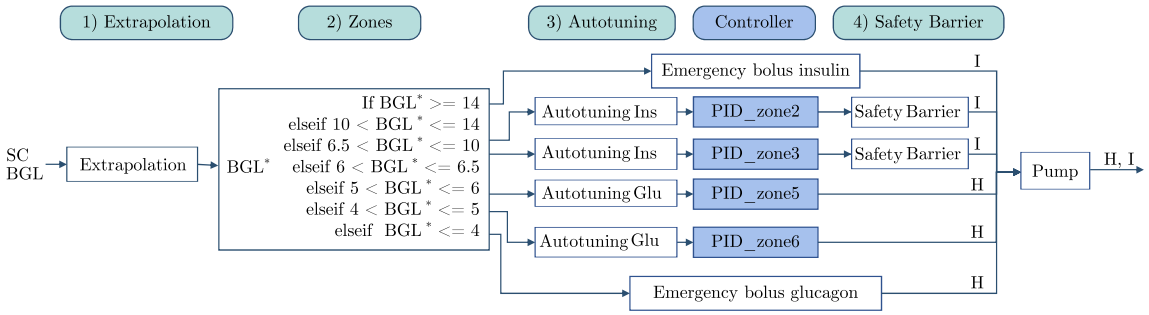

Fig. 4: Detailed block diagram of the two-layer PID controller. The white color denotes the supervisory layer, whereas the blue color represents the primary layer. The four strategies are displayed: (1) Extrapolation. (2) Division into zones. (3) Auto-Tuning. (4) Safety Barrier. As in Fig. 1 shown, the input is the subcutaneous blood glucose level (SC BGL), the extrapolated BGL is presented as BGL*, glucagon (H) and insulin (I) are determined during the process and outputted in the end.

A. Extrapolation of Sensor Data

SC sensors measurements lag behind the real BGL value due to physiological delays and their slow dynamics [19]. We implement the linear extrapolation method in the supervisory layer to predict the BGL in the next step and compensate for the sensor delay.

B. Zones

The first stage of the supervisory layer of the controller splits the BGL into seven zones, as shown in Fig. 5. In zones 1, 2, and 3, insulin is injected, and in zones 5, 6, and 7, glucagon is injected. Zone 4 is called the "quiet" zone, where no controller is activated so that neither insulin nor glucagon can be injected. The first and the last zone are the emergency zones, where in zone 1, an insulin bolus is given, and in zone 7, a glucagon bolus is injected. In total, a PID controller with four sets of coefficients is implemented, two for the injection of each hormone. Zones 2 and 6 consist of a more aggressively tuned PID controller, whereas zone 3 and 5 have a less aggressively tuned PID controller, both for insulin and glucagon respectively. Each zone has a separately chosen setpoint to allow a smooth transition into the next zone. To ensure safety, we opted for a target blood glucose level (BGL) of 6.4 mmol/l. BGLs below this level, falling into zones 4-7, are classified as low BGL. In such cases, no insulin is given to allow the BGL to return to the baseline.

C. Auto-Tuning PID controllers

To achieve an optimal performance of the designed PID, we implement a real-time auto-tuning stage to tune the PID controller for different individuals and scenarios. This is done by predicting the BGL for N_p samples using the individually identified meta-model [13] for each subject and then minimizing the quadratic error of the predicted BGL with the reference BGL value. The reference BGL value is selected according to the active zone as provided in the previous section. The decision variables in the optimization process are the PID coefficients. Notably, this procedure is done online and at every sampling time for zones 2,3,5 and

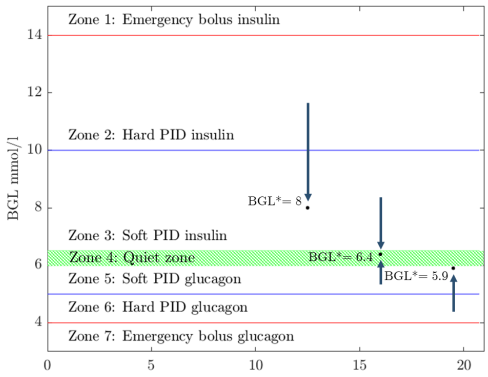

Fig. 5: Division of the BGL into 7 zones with different control types and actions. The borders of each zone as well as the setpoints (BGL*) are illustrated.

6. As explained in the previous section, the reference BGL is defined separately for the different zones. The cost function designed for this end is defined as follows:

$$c = \sum_{i=1}^{N_p} (G_i^* - G_{SC,i})^2, \tag{3}$$

where N_p is the prediction horizon, and at time k, c is the cost for the prediction interval $[k, k+N_p]$, G^* is the defined reference BGL for the current zone, and $G_{SC,i}$ is the i step ahead prediction of the BGL using the animal model at time $k+i$. In order to estimate the future BGL, a glucose infusion rate is needed. Here, for the zones 2 and 3 we assumed that the future glucose infusion rate equals the basal glucose infusion rate (see Section II-B). In contrast, to achieve a pessimistic prediction, a zero glucose infusion rate is assumed for the zones 5 and 6 (where the glucagon must be given).

The optimization problem can have multiple local minima, resulting in sub-optimal solutions. In order to address this

issue, the initial values given to the optimizer must be chosen carefully. In this paper, we choose the initial values using a trial-and-error method performed in multiple simulations for each zone. In addition, the decision variables are constrained in different zones to control the aggressiveness of the PID controller. The selected boundaries and the initial values are shown in Table I. The interior-point method is used to minimize the designed cost function (3).

TABLE I: Initial values and boundaries of the PID controller coefficients for different zones. The values are given in the format [K_p, K_i, K_d].

Zone	Initial Value	Lower Boundary	Upper Boundary
2	[0.2, 0, 5]	[0.1, 0, 1]	[0.5, 0, 20]
3	[0.1, 0, 2]	[0.01, 0, 0.02]	[0.2, 0, 10]
5	[-0.5, -0.01, -8]	[-5, -0.01, -10]	[-0.1, 0, -0.1]
6	[-1, -0.01, -5]	[-10, -0.01, -30]	[-1, 0, -5]

D. Safety Barriers

The BGL slope is one of the factors we need to consider for patient safety since if insufficient glycogen is stored in the liver, a rapid BGL drop can result in a hypoglycemic event. Thus, if the slope value exceeds a "dangerous value", the designed controller will be turned off to prevent excessive insulin. Since insulin is only given in zones 2 and 3, this is the only place where this safety barrier is needed. The threshold for the slope must be tuned based on the zone.

Furthermore, due to the pharmacokinetics and pharmacodynamics of the IP insulin, the half-life time of insulin is 60–100 minutes for IP injections [13]. In other words, the maximum effect of insulin and maximum drop in BGL appear 60–100 minutes after injection. Therefore, to prevent a rapid decrease in BGL in the next 60–100 minutes, additional safety parameters are used in zones 2 and 3 to stop the controller from giving more than a specified amount of insulin. The threshold for the amount of insulin must be chosen according to the body weight, sensitivity to insulin, and based on the active zone.

For example, for the pigs with 36 kg of body weight, the "dangerous slope" is defined as less than -0.01 mmol/L/min and 0 mmol/L/min for zones 2 and 3, respectively. In addition, the maximum amount of insulin that can be injected over a rolling time window of 60 min is set to 1.5 U for zone 2 and 2 U for zone 3. These values are chosen using a trial-and-error method in the simulations represented in the paper.

IV. Performance Measures

In order to evaluate the performance of the proposed control structure, three metrics are defined as follows:

A. Metric 1, Time in Range (TIR)

The Time in Range (TIR) is the first metric used to assess the controller's performance, indicating the duration for which the BGL remains in the desired range. Table II provides the ideal range, hyperglycemia levels, and hypoglycemia levels specified by the American Diabetes Association. Evaluating the effectiveness of treatments using Time above Range (TAR, hyperglycemia) and Time below Range (TBR, hypoglycemia) is also recommended [1, Chapter 6].

TABLE II: Glycemic targets for adults according to the American Diabetes Association [1, Chapter 6].

Ranges	BGL range [mmol/L]	Target [%]	Target [Time/Day]
Level 2 hyperglycemia	>13.9	<5	1h 12min
Level 1 hyperglycemia	10.1 - 13.9	<25	6h
Time in range	3.9 - 10.0	>70	16h 48min
Level 1 hypoglycemia	3.0 - 3.8	<4	58min
Level 2 hypoglycemia	<3.0	<1	14min

These glycemic targets can be formulated as

$$T = \frac{\sum_{i=1}^{N} \mathcal{I}_i}{N_s} \text{with } \mathcal{I}_i = \begin{cases} 1 \text{ for } G_i \in Range \\ 0 \text{ else} \end{cases} \tag{4}$$

with N_s the total number of steps, T as the resulting target value for each zone, which depends on the current step i, has to meet a condition based on the BGL value G_i and the ranges defined in Table II. This produces five different values for the zones. It should be noted that the BGL ranges are defined for humans, while the simulator used in this study is based on pig data.

B. Metric 2, Amount of Used Insulin and Glucagon

The second metric measures the control energy. For this, the used amount of insulin and glucagon is calculated to check how much control input was needed to control the BGL. Additionally, these values are used as an indicator, if enough insulin is injected and if the requirement is met that as little glucagon as possible is injected. This yields

$$X_{used} = \sum_{i=1}^{N} X_i \tag{5}$$

where X denotes the placeholder for insulin I and glucagon H. X_{used} is the amount of hormone used over the simulation time, N the total number of control intervals, and X_i the amount of injected hormone at each sampling interval i.

C. Metric 3, Severity of Hyperglycemia and Hypoglycemia

To compare the severity of hypoglycemia and hyperglycemia with different controllers or setups, we consider the integral of the BGL above or below the defined BGL thresholds. This threshold is chosen to be $G_{b,he} = 10$ mmol/L for hyperglycemia and $G_{b,ho} = 3.9$ mmol/L for hypoglycemia. We defined the severity of hyperglycemia [min·mmol/L] as follows.

$$S_{he} = \frac{area}{n_{aB}} = \frac{Q_U(G) - Q_{U,b}}{n_{aB}} \tag{6}$$

where G is the BGL, n_{aB} in the number of the samples that $G > G_{b,he}$, $Q_U(G)$ is integral of the BGL values exceeding $G_{b,he}$, and $Q_{U,b} = G_{b,he} \cdot n_{aB} \cdot \Delta T$, in which ΔT is the sampling time. Similar to S_{he}, the severity of hypoglycemia is defined as follows.

$$S_{ho} = \frac{Q_L(G_{b,ho}) - Q_{L,b}}{\bar{n}_{bB}} \tag{7}$$

where $\bar{n}_{bB}$ is the number of the samples that $G < G_{b,ho}$, $Q_L(G)$ is integral of the BGL values less than $G_{b,he}$, and $Q_{L,b} = G_{b,ho} \cdot \bar{n}_{bB} \cdot \Delta T$.

V. Results

This section presents the results of the proposed control approach in different scenarios. For a detailed evaluation, we show the effect of having each of the proposed stages of the supervisory layer (extrapolation, zones, auto-tuning, safety barriers), which are added one by one, yielding the final controller with all implemented stages in the end. As explained in section II, the parameters of the simulator are identified using the animal experiment conducted on anesthetized pigs. Then, the effectiveness of the safety barriers and the zone PID with auto-tuning is assessed on other subjects using the proposed metrics.

In order to challenge the controller, four sets of $\{\alpha_1, \alpha_2, ..., \alpha_5\}$ are identified from four animal experiments, and the designed controller is performed on them in the simulator. In addition, three sets of extended simulations with time-varying sensitivity values $(\alpha_2, \alpha_3, \alpha_4)$ are done on each of them, resulting in 16 simulations in total. In the extended simulations, $\alpha_2, \alpha_3, \alpha_4$ are changing in the sinusoidal shape with three neutral positions (max, cen, and min) explained in Section II-A. The effectiveness of the proposed stages in the designed structure is evaluated in the following sections.

A. Development Stages

As shown in Fig. 4, the input of the controller is represented by the sensor value. In order to compensate the delay, sensor data is extrapolated by predicting a future step. Fig. 6 shows an approximation of the extrapolated BGL value to the actual BGL using the delayed sensor. It can be easily seen that the extrapolated and actual BGL have almost the same sinusoidal peaks.

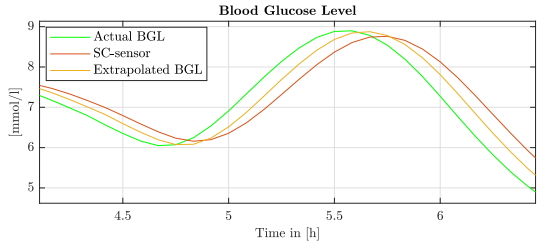

Fig. 6: Extrapolation reduces the time lag of the SC sensors.

A PID controller is chosen as a comparison control structure, which has the same tuning as zone 3 for insulin infusions and the same tuning as zone 5 for glucagon infusions. However, the reference BGL for this single-layer PID is set to 7 mmol/L (middle point of the desired range of 3.9–10 mmol/L) to avoid problems with hypoglycemia. The effect of the control scheme stages can be seen in Fig. 7, 8 and 9. When looking at Fig. 7, the first stage of the two-layer controller injects slightly larger amounts of insulin, and the transition between injecting the hormones is characterized by small pauses, compared to the single-layer controller.

Auto-tuning significantly increases the use of the control input, which, however, can also considerably decrease the average of the BGL (Fig. 8 and 9). The maximum BGL is noticeably reduced, while the minimum BGL is increased. It is important to note that these are average values of the results of 16 simulations. This reduction in the range of the BGL is also evident from Fig. 7, where the increased aggressiveness of the controller is noticeable from the inputs.

The increase in aggressiveness due to auto-tuning is also noticeable in an increase in hypoglycemic events. Therefore, the safety barrier is implemented for zone 2. This method shows a negligible effect on the total avoidance of hypoglycemic events and reduction of insulin usage. In contrast, when implemented in zones 2 and 3, the amount of insulin can be significantly reduced. This also reduces the need for glucagon injections. However, the activation of safety barrier for both zones leads to a renewed slight increase in the average and maximum BGL. The increased course of BGL is also evident from Fig. 7.

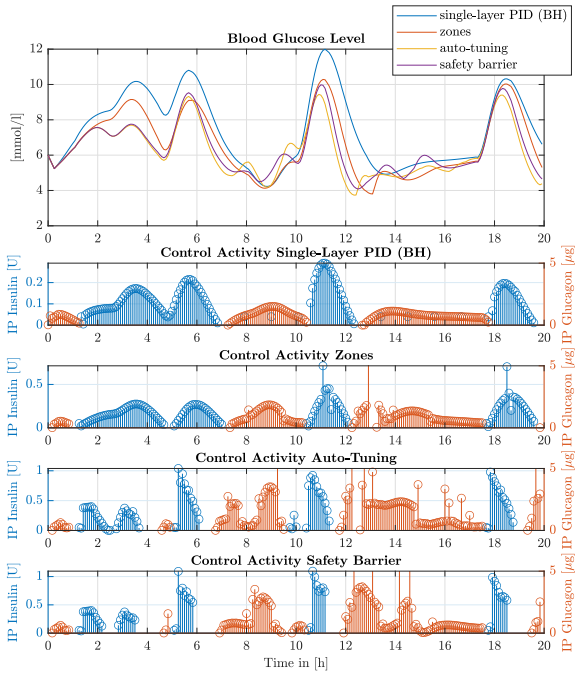

Fig. 7: Comparison of BGL course in 3 stages of proposed 2-layer PID controller (added incrementally) with a single-layer bi-hormonal (BH) PID controller (tuned like zones 3 and 5 of 2-layer). Zones denote 2nd stage, auto-tuning is 3rd, and safety barrier is 4th (activated for zones 2 and 3). Extrapolation is implemented for each stage since it represents the first stage. Subplots show insulin and glucagon control input for each stage.

B. Final Controller

The proposed PID controller includes auto-tuning, time delay compensation through extrapolation, zone-based switch-

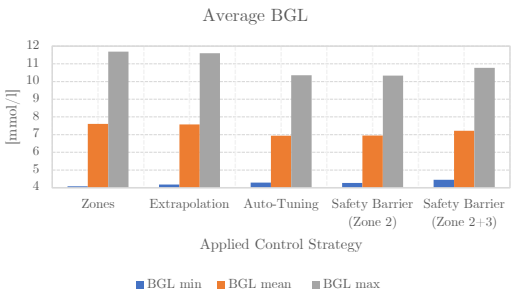

Fig. 8: Comparison of the minimum, average and maximum BGL over the different stages.

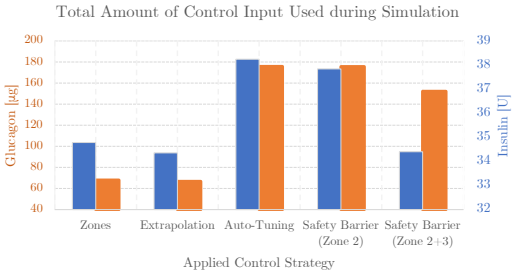

Fig. 9: Course of the control inputs insulin and glucagon over the different development stages of the controller (averaged for the 16 simulations).

ing, and a safety barrier to limit BGL rate. Table III shows the performance of the final PID controller for different sensitivity settings. L2 hypoglycemia and L2 hyperglycemia can be avoided except for the constant sensitivity setting. When considering the TIR, a crucial dependence of the effectiveness of therapy on sensitivity is also apparent. Despite an increase in the amount of insulin, the greatest proportion of hyperglycemia occurs for the minimum sensitivity. With an increase in sensitivity, the TIR and the necessary amount of glucagon increases, while maximum sensitivity achieves the smallest BGL range and mean.

For the constant sensitivity values, one data set has the lowest sensitivity values, leading to hypoglycemic events. Away from this, less insulin but more glucagon is used, which results otherwise in the range of the other sensitivity values.

Fig. 10 shows the comparison of the results when the saw-tooth profile and the sinusoidal profile are evaluated. Here, the sawtooth profile shows stronger irregularities, which is due to the fast and abrupt change of the sensitivities. This means that the extremes are stronger, although they are still within a satisfactory range.

VI. Discussion

The supervisory layer's extrapolation compensates for sensor time delay, resulting in a slight minimum BGL increase and maximum BGL reduction. The zone stage improves glycemic control, as evident from Fig. 7. However, this improvement comes with the cost of more tuning parameters

TABLE III: Performance metrics (averaged over different data sets): The settings min, cen, and max correspond to the sinusoidal settings, described in Eqs. (2a)–(2c). The constant setting (con) represents the time-invariant sensitivity values. L1 describes regular hyperglycemia or hypoglycemia events, whereas L2 describes severe events. $N(S_{he})$ and $N(S_{ho})$ represent the number of hyperglycemic and hypoglycemic events.

	Overall	**Min**	**Cen**	**Max**	**Con**
L2_hyper [%]	0.00	0.00	0.00	0.00	0.00
L1_hyper [%]	6.57	17.66	5.75	0.91	1.94
TIR [%]	92.51	82.34	94.25	99.09	94.35
L1_hypo [%]	0.93	0.00	0.00	0.00	3.71
L2_hypo [%]	0.00	0.00	0.00	0.00	0.00
I [U]	34.40	42.47	33.86	31.49	29.78
H [μg]	152.25	77.81	100.51	151.50	279.17
S_{he} [min·mmol/L]	0.53	0.87	0.30	0.35	0.48
$N(S_{he})$	1.50	2.50	2.25	0.50	0.75
S_{ho} [min·mmol/L]	0.07	0.00	0.00	0.00	0.28
$N(S_{ho})$	0.19	0.00	0.00	0.00	0.75
min(BGL) [mmol/L]	4.44	4.70	4.66	4.35	4.07
meanBGL) [mmol/L]	7.22	8.10	7.34	6.82	6.63
max(BGL) [mmol/L]	10.78	11.89	10.74	10.12	10.36

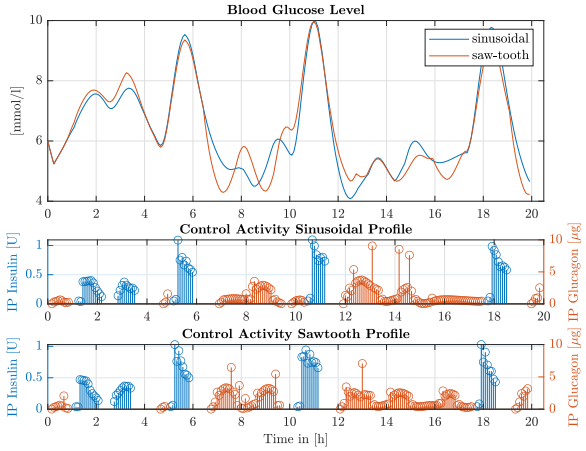

Fig. 10: A final evaluation of the performance of the final controller where the controller is applied to the two different sensitivity profiles, where the insulin sensitivity and the glucagon sensitivity are time-variant as a sinusoidal or a saw-tooth function. Apart from the sensitivity profiles everything is identical.

and the complexity of the controller. The tunable parameters must be studied in detail, and sensitivity analysis of the controller to these parameters should be done before implementing the designed method in practice, which is kept for future work. In addition, a high-gain observer can be incorporated with the controller for better functionality and safer control, as discussed in [20], [21]. Auto-tuning adjusts PID parameters automatically for different individuals and scenarios with time-varying settings, resulting in reduced minimum and average BGL for all individuals. However, increased aggressiveness can lead to undershoots close to the lower limit. A penalty could be added to the cost function

to limit hormone use, but this is not included in the current simple cost function. Improvements to the auto-tuning stage are left for future work. The safety barriers in zone 2 and 3 terminate insulin injections early, thus reducing the impact of increased aggressiveness and control activity from auto-tuning. Consequently, there is a significant increase in the minimum BGL, but at the cost of a decrease in mean BGL and some slight hyperglycemic events.

It is important to note that glucagon is an unstable liquid that can cause blockage of the infusion set and the pump. However, in real experiments, we suggest changing the glucagon infusion set every 24 hours similar to [22].

Overall, the proposed control structure meets the requirements specified in Table II. However, the controller's effectiveness is heavily influenced by insulin and glucagon sensitivities. Despite the saw-tooth profile's discontinuities, it produces satisfactory control results. The enhanced performance and safety of the controller are achieved at the cost of increased complexity and tuning parameters compared to the single-layer PID controller.

VII. Conclusion

This paper proposes a two-layer PID controller with four stages to improve glycemic control. The controller compensates for sensor delay, prevents on-off behavior, adjusts PID coefficients automatically, and adds safety barriers to avoid hypoglycemia. Auto-tuning predicts future BGL, making the structure comparable to MPC approaches and computationally efficient for real-time use. The proposed controller is effective on a complex and well-tuned simulator based on an animal model, achieving satisfactory results despite time-varying insulin and glucagon sensitivities. Future studies can evaluate the framework on a human-based simulator to determine if similar outcomes can be achieved without requiring meal announcements.

VIII. Acknowledgments

This research is funded by the Research Council of Norway (project no. 248872) and the Centre for Digital Life Norway. We want to thank Professor Sven Magnus Carlsen and Professor Herbert Werner for the discussions.

References

[1] American Diabetes Association, "Introduction: Standards of medical care in diabetes—2021," *Diabetes Care*, vol. 44, no. Supplement_1, pp. S1–S2, Dec. 2020.

[2] Y. Ho, *Patient-Specific Controller for an Implantable Artificial Pancreas*. Springer-Verlag GmbH, 2018. [Online]. Available: https://www.ebook.de/de/product/34256288/yvonne_ho_patient_specific_controller_for_an_implantable_artificial_pancreas.html

[3] C. Toffanin, L. Magni, and C. Cobelli, "Artificial pancreas: In silico study shows no need of meal announcement and improved time in range of glucose with intraperitoneal vs. subcutaneous insulin delivery," *IEEE Trans. Med. Robot. Bionics*, vol. 3, no. 2, pp. 306–314, 2021.

[4] P. A. Bakhtiani, L. M. Zhao, J. El Youssef, J. R. Castle, and W. K. Ward, "A review of artificial pancreas technologies with an emphasis on bi-hormonal therapy," *Diabetes, Obesity and Metabolism*, vol. 15, no. 12, pp. 1065–1070, 2013.

[5] K. von der Saal, *Biochemie*. Springer Berlin Heidelberg, 2020. [Online]. Available: https://www.ebook.de/de/product/38050241/karin_von_der_saal_biochemie.html

[6] R. Gondhalekar, E. Dassau, and F. J. Doyle III, "Periodic zone-mpc with asymmetric costs for outpatient-ready safety of an artificial pancreas to treat type 1 diabetes," *Automatica*, vol. 71, pp. 237–246, 2016.

[7] R. Gondhalekar, E. Dassau, and F. Doyle III, "Velocity-weighting & velocity-penalty mpc of an artificial pancreas: Improved safety & performance," *Automatica*, vol. 91, pp. 105–117, 2018.

[8] E. Matamoros-Alcivar, T. Ascencio-Lino, R. Fonseca, G. Villalba-Meneses, A. Tirado-Espin, L. Barona, and D. Almeida-Galarraga, "Implementation of MPC and PID control algorithms to the artificial pancreas for diabetes mellitus type 1," in *2021 IEEE International Conference on Machine Learning and Applied Network Technologies (ICMLANT)*. IEEE, Dec. 2021.

[9] F. Tang and Y. Wang, "Design of bi-hormonal artificial pancreas system using switching economic model predictive control," in *2017 36th Chinese Control Conference (CCC)*. IEEE, Jul. 2017.

[10] R. W. Jones, "Glucagon control strategies for the bi-hormonal artificial pancreas," in *IEEE Conf. Ind. Electr. Appl. (ICIEA)*. IEEE, Jun. 2019.

[11] N. Taleb, A. Quintal, R. Rakheja, V. Messier, L. Legault, E. Racine, and R. Rabasa-Lhoret, "Perceptions and expectations of adults with type 1 diabetes for the use of artificial pancreas systems with and without glucagon addition: Results of an online survey," *Nutrition, Metabolism and Cardiovascular Diseases*, vol. 31, no. 2, pp. 658–665, Feb. 2021.

[12] L. M. Huyett, E. Dassau, H. C. Zisser, and F. J. Doyle III, "Design and evaluation of a robust pid controller for a fully implantable artificial pancreas," *Industrial & engineering chemistry research*, vol. 54, no. 42, pp. 10 311–10 321, 2015.

[13] K. D. Benam, H. Khoshamadi, M. K. Åm, Ø. Stavdahl, S. Gros, and A. L. Fougner, "Identifiable prediction animal model for the bi-hormonal intraperitoneal artificial pancreas," *Journal of Process Control*, vol. 121, pp. 13–29, 2023.

[14] C. Lopez-Zazueta, A. L. Fougner *et al.*, "Low-order nonlinear animal model of glucose dynamics for a bihormonal intraperitoneal artificial pancreas," *IEEE Trans. Biomed. Eng.*, no. 3, pp. 1273–1280, Mar. 2022.

[15] A. Chakrabarty, J. M. Gregory, L. M. Moore, P. E. Williams, B. Farmer, A. D. Cherrington, P. Lord, B. Shelton, D. Cohen, H. C. Zisser *et al.*, "A new animal model of insulin-glucose dynamics in the intraperitoneal space enhances closed-loop control performance," *Journal of Process Control*, vol. 76, pp. 62–73, 2019.

[16] M. Halvorsen, K. D. Benam, H. Khoshamadi, and A. L. Fougner, "Blood glucose level prediction using subcutaneous sensors for in vivo study: Compensation for measurement method slow dynamics using kalman filter approach," in *2022 IEEE 61st Conference on Decision and Control (CDC)*. IEEE, 2022, pp. 6034–6039.

[17] B. Koletzko, O. Goulet, J. Hunt, K. Krohn, R. Shamir, and the Parenteral Nutrition Guidelines Working Group, "Guidelines on paediatric parenteral nutrition: 5. Carbohydrates," *Journal of Pediatric Gastroenterology & Nutrition*, vol. 41, no. Supplement 2, pp. S28–S32, Nov. 2005.

[18] C. Dalla Man, M. Camilleri, and C. Cobelli, "A system model of oral glucose absorption: validation on gold standard data," *IEEE Trans. Biomed. Eng.*, vol. 53, no. 12, pp. 2472–2478, 2006.

[19] Ø. Stavdahl, A. L. Fougner, K. Kölle, S. C. Christiansen, R. Ellingsen, and S. M. Carlsen, "The artificial pancreas: A dynamic challenge," *IFAC-PapersOnLine*, vol. 49, no. 7, pp. 765–772, 2016.

[20] K. D. Benam, H. Talebi, and M. A. Khosravi, "Full order high gain observer design for image-guided robotic flexible needle steering," in *2019 27th Iranian Conference on Electrical Engineering (ICEE)*. IEEE, 2019, pp. 1151–1156.

[21] K. D. Benam, H. Khoshamadi, L. Lema-Pérez, S. Gros, and A. L. Fougner, "A nonlinear state observer for the bi-hormonal intraperitoneal artificial pancreas," in *2022 44th Annual International Conference of the IEEE Engineering in Medicine & Biology Society (EMBC)*. IEEE, 2022, pp. 171–176.

[22] H. Blauw, A. J. Onvlee, M. Klaassen, A. C. van Bon, and J. H. DeVries, "Fully closed loop glucose control with a bihormonal artificial pancreas in adults with type 1 diabetes: an outpatient, randomized, crossover trial," *Diabetes Care*, vol. 44, no. 3, pp. 836–838, 2021.